# BIOMEDICAL APPLICATIONS OF HOLOGRAPHY

The three-dimensional imaging property and great depth of field immediately suggest applications such as population studies in large tanks. Less obvious applications based on optical filtering rather than imaging include diagnostic cytology and radiology.

ERNEST J. FELEPPA

WITH THE SIMPLICITY of its fundamental theory and the simplicity of its application, holography is an elegant concept. Moreover it is versatile, being applicable to a variety of imaging and nonimaging problems. Holography certainly warrants serious consideration by biological and medical researchers as a valuable addition to the list of physical techniques that have become essential to them.

Two of the possible applications are improved resolution in radiography and faster, more accurate diagnostic cytology. In radiography the requirement of a geometrically small source (ideally a "point source") could be abandoned, and resolution improved. Shorter exposures and three-dimensional analysis are additional advantages. And in diagnostic cytology (the detection of cancer by the identification of malignant cells) hours of laborious work at the microscope could be saved, and the identification of cells made more efficient, with a holographic filter technique. Vidicon scanning and computer analysis would make preliminary inspection automatic; only those cells picked out as "suspect" would need to be examined and evaluated by the operator.

# HOLOGRAPHY THEORY

Holography has become a fairly familiar term to scientists. To most it means a technique of forming three-dimensional images. Indeed it is that, but three-dimensional images are only one consequence of holography's more fundamental ability to reconstruct a wave. 1-5 Holography can also func-

tion in a nonimaging sense where it acts as a complex spatial filter.<sup>6</sup> Although holography can be defined in an imaging sense as a method for recording and reconstructing an object-scattered wave, it is more completely defined as a method of complex, spatial filtering.

# Recording

A hologram is a recording of an interference pattern. In imaging applications, a reference wave is superimposed upon an object-scattered wave. Because the interference depends upon the relative amplitudes and phases of the two waves, coherent illumination must be used to keep the phase relationships constant during recording. Knowledge of the amplitude and phase of one wave, the reference wave, subsequently yields the amplitude and phase of the other.3 For simplicity the reference wave is plane or spherical. If we describe the reference wave by U1 and the object-scattered wave by U2, the superposition of U1 and U2 in the x-y plane produces a wave U1 + U2 (figure 1a). The recording in the x-y plane will record the intensity I of this wave

$$I(x,y) = (\mathbf{U}_1 + \mathbf{U}_2)(\mathbf{U}_1 + \mathbf{U}_2)^*$$
  
=  $|\mathbf{U}_1|^2 + |\mathbf{U}_2|^2 + \mathbf{U}_1\mathbf{U}_2^*$   
+  $\mathbf{U}_1^*\mathbf{U}_2$  (1)

where an asterisk indicates the complex conjugate. In equation 1, the relevant, signal-bearing terms are  $U_1$   $U_2^*$  and  $U_1$   $U_2$ .

## Emulsion response

The amplitude transmission T of a photographic emulsion (the usual re-

cording medium) exposed to an intensity I for a time t is  $^7$ 

$$T = E^{-\gamma/2}$$

where E is the exposure, It, and  $\gamma$  is the slope of the emulsion response curve in figure 2. The factor 1/2 appears in the exponent because we are concerned with amplitude and not intensity, the square of the amplitude. Thus

$$T = (It)^{-\gamma/2}$$

and

$$T \propto I^{-\gamma/2}$$

for constant t.

Thus, the superposition of  $\mathbf{U}_1$  and  $\mathbf{U}_2$  is recorded as

$$T = (|\mathbf{U}_1|^2 + |\mathbf{U}_2|^2 + \mathbf{U}_1\mathbf{U}_2^* + \mathbf{U}_2\mathbf{U}_1^*)^{-\gamma/2}$$
  
=  $(s_0 + s)^{-\gamma/2}$ 



Ernest J. Feleppa took his bachelor's degree at Cornell University in physics and his doctorate at Columbia University in biophysics. Still at Columbia, he is currently working on genetic control of neuronal connections in Daphnia and has just started a collaboration with New York Hospital on holography applied to studies of the eye.

where  $s_0 \equiv |\mathbf{U}_1|^2 + |\mathbf{U}_2|^2$  and  $s \equiv \mathbf{U}_1$  $\mathbf{U}_2^* + \mathbf{U}_2 \mathbf{U}_1^*$ . Then expanding

$$T = s_0^{-\gamma/2} + (-\gamma/2) s_0^{(-\gamma/2)-1}s + \frac{[-\gamma/2][(-\gamma/2)-1]}{2!} s_0^{(-\gamma/2)-2}s^2 + \dots + \frac{(-\gamma/2)!}{[(\gamma/2)-k]k!} s_0^{-(\gamma/2-k)}s^k + \dots$$
 (2)

If  $s \ll s_0$ 

$$T \bowtie s_0^{-(\gamma/2)} + (-\gamma/2)s_0^{(-\gamma/2)}s$$

We may rewrite this equation as

$$T \bowtie A + Bs$$

where  $B \equiv (-\gamma/2)s_0^{(-\gamma/2)-1}$  and  $A \equiv s_0^{-\gamma/2}$ . Thus  $s_0$  must be large compared to s to utilize the linear portion of the response curve without signal excursions into the nonlinear portions, and to supress high-order terms in the expansion of equation 2. However, if recording is limited to the linear portion of the response curve and if  $\gamma = 2$ , the amplitude transmission will simply be the inverse of the exposure. This restriction is necessary only in certain filtering applications, concerned with image analysis, to be discussed later.

### Reconstruction

Illumination of the recording with a third wave,  $\mathbf{U}_3$  (figure 1b), will produce a wave  $\mathbf{U}_4$  modulated by the hologram

$$\mathbf{U}_4 = \mathbf{U}_3 T$$
$$= \mathbf{U}_3 (A + Bs)$$

Considering only s, the signal portion of the recording,

$$\mathbf{U}_4 = \mathbf{U}_3 \, \mathbf{U}_1 \, \mathbf{U}_2^* + \mathbf{U}_3 \, \mathbf{U}_1^* \, \mathbf{U}_2 \quad (3)$$

If the reconstructing wave U3 is identical to the reference wave U1, the second term in equation 3 becomes a constant times U2. Thus, the objectscattered wave is reconstructed. The first term on the right-hand side of equation 3 is more simply discussed by considering U1 and U3 to be plane waves; then  $U_1 = U_1^*$ , and the first term is a constant times the complex conjugate of U2. In other words, when plane reference and reconstructing waves are used, a virtual and a real image are reconstructed, each with unit magnification. If identical spherical waves are used one image will be virtual with unit magnification, and one will be real with a magnification other than unity. If nonidentical reference and reconstructing waves

are used magnification is not unity, but it can be controlled by controlling the reconstructing-wave radius.

# Magnification

Expressions for magnification can be most simply derived by comparing a hologram to a Gabor zone plate<sup>8,9</sup> (see figure 3). Such a zone plate has two focal lengths, one positive and one negative. As shown in equation 3, a reconstructing wave identical to the reference wave will be diffracted by the hologram to form an image point in a position identical to its corresponding object point. Thus the focal length of the hologram for that point is

$$f = \pm z_1 z_2/(z_1-z_2)$$

where  $z_1$  is the axial distance from the reference source to the hologram, and  $z_2$  is the axial distance from the object source to the hologram. The axis is determined by the line joining the ref-

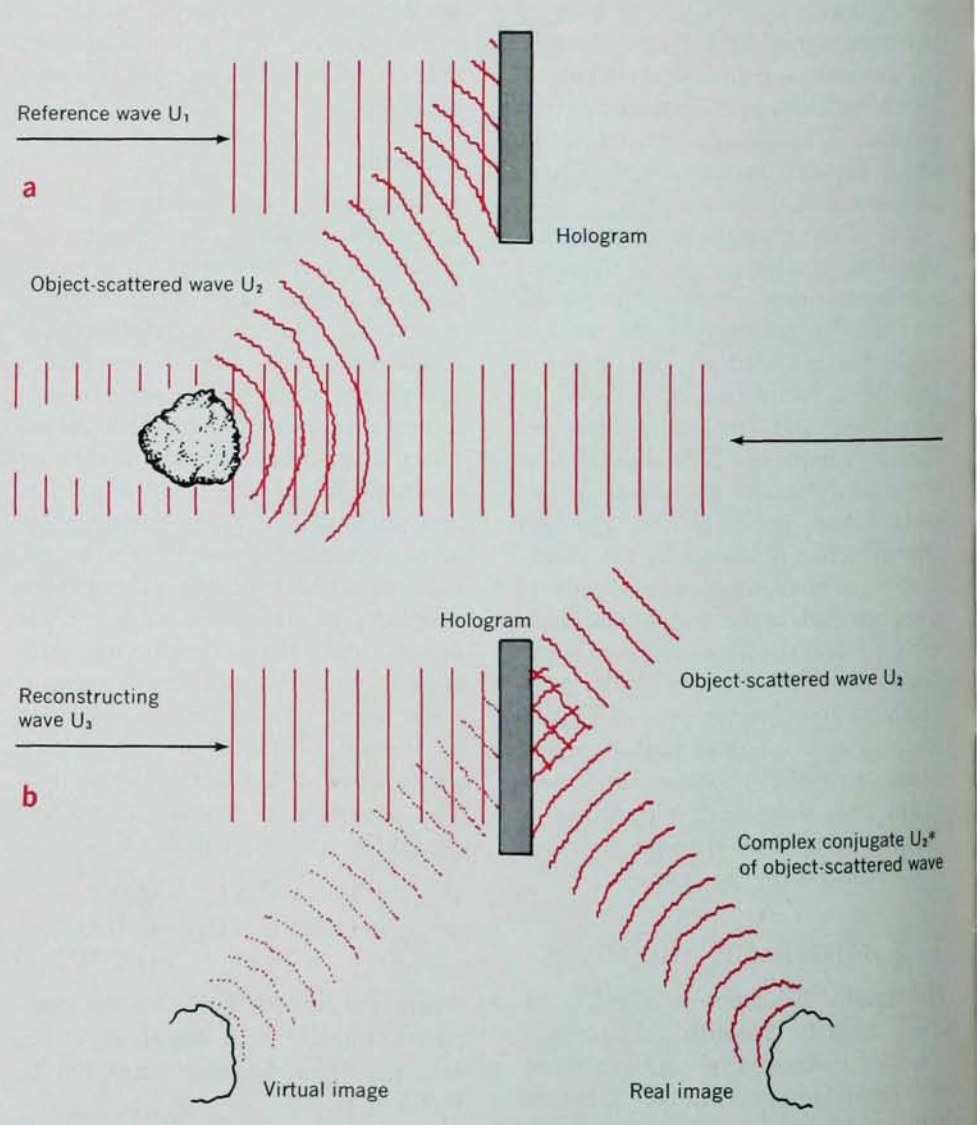
erence and object sources. If we define lateral magnification M as  $-z_4/z_2$ 

$$M = \mp 1/(\pm z_2 z_3^{-1} + z_2 z_1^{-1} - 1)$$
(4)

where  $z_3$  is the distance from the reconstructing source to the hologram, and  $z_4$  is the distance from the image to the hologram. In these expressions the z's are positive on the reference-source side of the hologram (the x-y plane). Positive magnification corresponds to a real image, negative magnification to a virtual image.

# Resolution

Resolution in a hologram is determined by the useful aperture of the hologram, often limited by the resolution of the recording medium. The aperture is determined at the radius where fringe spacing equals the resolution of the medium. When two waves are incident upon the record-



RECORDING AND RECONSTRUCTION. Top part (a) of figure shows how  $U_1$  (the reference wave) and  $U_2$  (scattered from the object) interfere to form the hologram. In lower part (b) the reconstructing wave  $U_3$  shines on the hologram. The hologram diffracts  $U_3$ , giving rise to a real and a virtual image.

ing plane at angles  $\theta_1$  and  $\theta_2$ , the spacing of the resultant interference fringes (see figure 3) is  $\lambda/(\sin\theta_2-\sin\theta_1)$ . If the recording resolution is  $\epsilon$ , the aperture is defined when  $\sin\theta_2=(\lambda+\epsilon\sin\theta_1)/\epsilon$ . With the conventional expression for microscope resolution,  $\xi=1.22~\lambda/n\sin\theta$ , the resolution of the system is

$$\xi = 1.22\lambda\epsilon/n(\lambda + \epsilon \sin\theta_1)$$

where n is the refractive index of the space between the object and the hologram. If the reference wave is plane,  $\theta_1$  is 0, and  $\xi$  is approximately  $\epsilon$ . On the other hand, if the object source is very close to the reference source,  $\sin\theta_1 \bowtie \sin\theta_2$  and fringe spacing will be large. The aperture then will not be limited by the resolution of the recording medium, but rather by the physical dimensions of the medium.

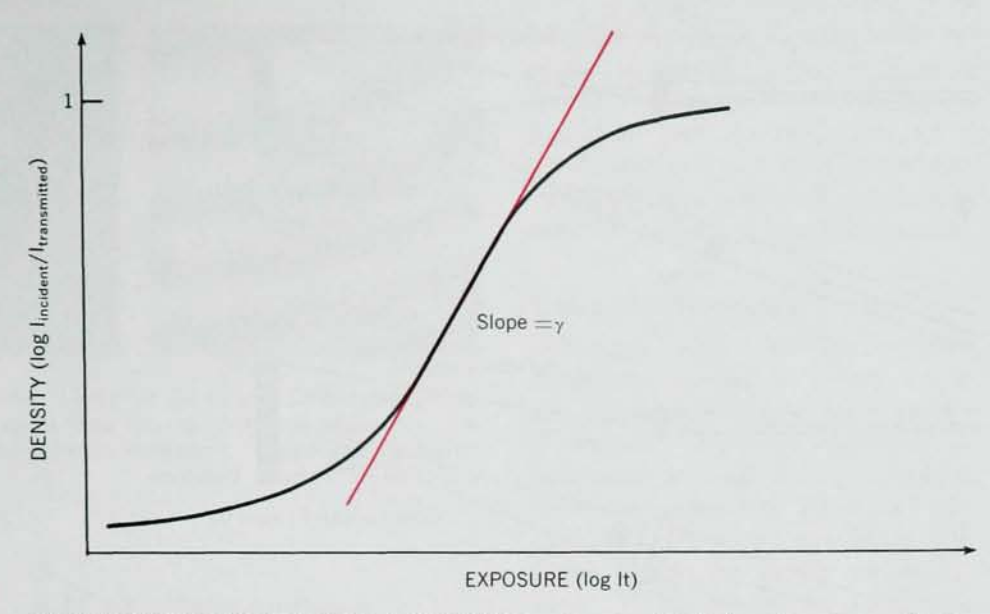
### IMAGING APPLICATIONS

Three-dimensional images are an important consequence of the reconstruction of the object-scattered wave. Because the entire wave is reconstructed, the complete amplitude and phase character of the object is retained. Retention of phase character permits the application of dark-field, phase-contrast and interference techniques to the reconstructed, bright-field image.

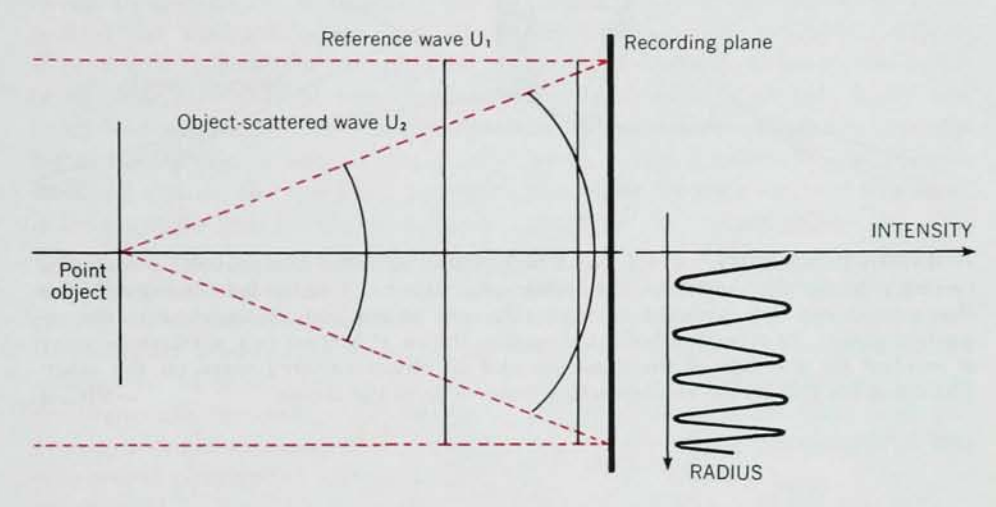
As holography records every plane in the specimen it is especially useful in biology, where dynamic, living systems are investigated. In such systems, conditions change with time and the ability of holography to record an infinite number of specimen planes simultaneously is a significant advantage over conventional techniques (figure 4). Some applications that come immediately to mind are the studies of populations in a pond or large tank, capillary-bed structure, the interior of the eye, phagocytosis, amoeboid motion and cell division.<sup>10</sup>

# Pseudoscopy

An interesting property of holographic real images is their pseudoscopy. Objects in the recorded scene that are nearest the hologram remain nearest the hologram in both the virtual and the real images. Thus, spatial relationships will appear normal in the virtual image; subjects near the observer will block the view of objects more distant. However, in the real image, those same objects near the recording plane are far from the ob-



PHOTOGRAPHIC-EMULSION RESPONSE. Density D (after development) increases with exposure E in such a way that  $D=\gamma \log E$  over part of the range; gamma is a constant with a value determined by the development. —FIG. 2



APERTURE of a recorded hologram. A point object and a collimated reference wave together produce an interference pattern consisting of a set of concentric circles, with spaces that decrease with increasing radius as shown in the intensity graph at right. Such a pattern is called a "Gabor zone plate." Maximal aperture of the hologram is determined by the resolution of the recording medium.

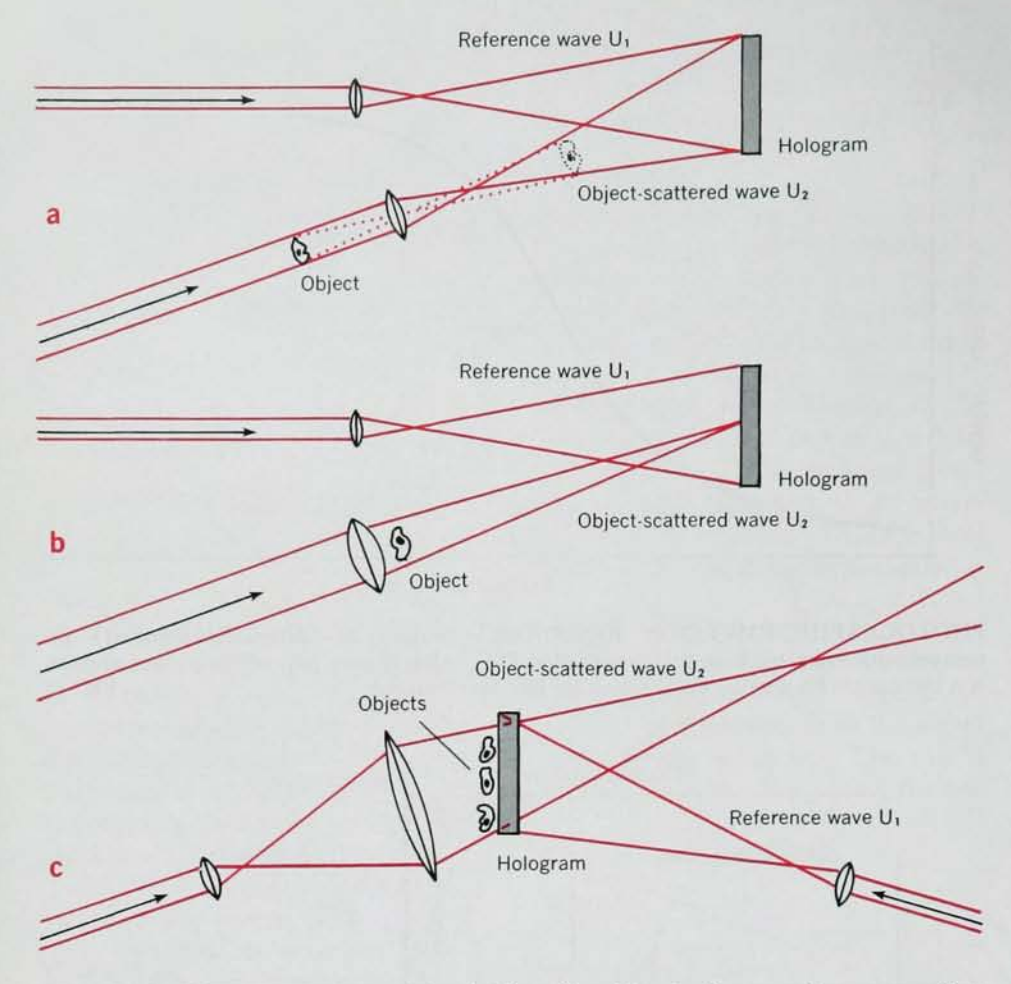
—FIG. 3

server but will block his view of nearer objects. Because depth is perceived by parallax as well as stereoscopy, the observer can simply shift his point of view of the real image to see objects nearer to him around objects that appear to be more distant. Despite this peculiarity of the real image, it is often the more convenient image to use for image manipulation or lensless photography.<sup>10</sup>

### Dark field and phase contrast

When a bright-field image is obtained, the image of the specimen-illuminating source can be manipulated to produce dark-field or phase-contrast images. 10.11.12 We can produce a dark-field image by placing an opaque stop at the image of the illuminating source, and a phase-contrast image by placing

a phase-retarding stop at this image. The illuminating-source image is obtained directly in the real-image wave. We obtain the source image in the virtual image with a lens, relocating the virtual images and making them real. This lens can be used to reverse the curvature of the reconstructing wave,11 or to reimage directly the virtual images. 10 An alternative is to place the illuminating source considerably further from the hologram than the reference source. Then, as shown by equation 4, if a reconstructingsource-hologram distance,  $z_3$ , equal to the reference-source-hologram distance,  $z_1$ , is used, M = -1 and -1/ $[(2z_2/a_3) - 1]$ . If the specimen is at approximately the same distance,  $z_2$ , from the hologram as the reference source, so that  $z_2' = z_3$ , the specimen



HOLOMICROGRAPHY. At top (a) a high-quality objective lens provides a magnified specimen image that serves as the holographic object. Fourier holomicrography, as shown in center (b), includes adjacent reference source and object, close to the recording plane. In reflection holomicrography, shown at bottom (c), a reference wave is incident on one side of the emulsion and an object-scattered wave on the other. The hologram reflects the reconstructing wave to form the image.

—FIG. 4

will have a magnification of -1 in both images, that is, it will be reconstructed as a virtual image in both diffracted waves. The illuminating source at z<sub>0</sub>" will also be reconstructed as a virtual image with M = -1 in one wave. However, in the other, if  $z_3$  is greater than  $2z_2''$ , M>0. That is, if the illuminating source  $z_2''$  is less than half as far from the hologram as the reference and reconstructing sources, it will be reconstructed as a real image. We can do this simply by illuminating the specimen with a wave converging to a point near the recording plane.

### Interference images

Interferometry is especially useful in biology, 13,14 and we can obtain holographic interference images in a variety of ways. From a single, bright-field hologram, finite- and infinite-fringe differential and duplication interference can be obtained. The simplest method for obtaining interfero-

grams is to doubly expose a single hologram<sup>10,14</sup> (figure 5). For duplication interference we make one exposure using the specimen, the second using a plane wave. For differential interference we make both exposures using the specimen. If the angle of incidence of the recorded waves is left unchanged between exposures, infinite-fringe interferograms will be formed. If the angle is changed, we get finite-fringe interferograms.

# Duplication interference

Infinite-fringe duplication interference provides contour maps of specimen optical thickness. For a sphere, a useful geometry to consider in biology, the difference between specimen and surround refractive indices is

$$(n - n_0) = \lambda r / [2S\sqrt{\rho^2 - r^2}]$$

where n is the specimen index,  $n_0$  is the surround index,  $\lambda$  is the wavelength of the illuminating light,  $\rho$  is the radius of the sphere, r is the radius

within the sphere at which S is measured and S is the spacing of the fringes in the specimen. This example is not useful for determining  $(n - n_0)$ , but it is the basis for the following example.

Finite-fringe duplication interference produces a set of parallel background fringes that are displaced as they pass through the images. Let us assume that the fringes are parallel to the *y* axis and the spherical specimen is centered on the origin, so that

$$(n - n_0) = \lambda D / [2S_0 \sqrt{\rho^2 - x^2}]$$

where D is the fringe displacement of a given fringe (relative to its position in the surround) measured at y=0. Then  $S_0$  is the fringe spacing in the surround, and x is the location of the fringe at y=0. Using this expression we can determine the refractive index of the specimen.

# Differential interference

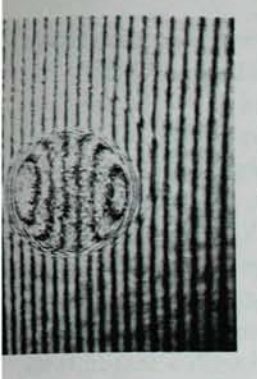
Differential infinite-fringe interference is useful primarily in obtaining contrast; we impart a small lateral displacement between exposures so that destructive interference occurs on one side of the specimen. It is also useful in detecting changes that occur between exposures; destructive interference occurs if a path length changes by  $\lambda/2$ . This technique is especially useful in scenes recorded by reflected illumination. A surface displacement less than  $\lambda/4$  can easily be detected.

We can use finite-fringe differential interference to measure refractive indices. A small angular and lateral displacement between exposures produces parallel fringes outside the specimen, and, within a spherical specimen, it produces fringes that are curved and displaced from the corresponding fringes in the surround. Index of refraction is determined by

$$(n - n_0) = \lambda D / \left\{ 2S_0 \left[ \sqrt{\rho^2 - (x - d)^2} - \sqrt{\rho^2 - (x + d)^2} \right] \right\}$$

for a displacement of 2d. Fringe identification is unequivocal because the fringe at x=0 is not displaced. If  $n>n_0$  the fringes within the specimen are displaced away from the y axis; if  $n< n_0$  they are displaced towards the y axis.

Although double-exposure interferometry is simple, it is inflexible; fringe spacings, fringe displacements and specimen displacements are determined by the manipulation effected between exposures. More flexible methods employ singly exposed holo-







INTERFERENCE of microscope images is shown here for the eggs of Lytechnius pictus. At left is differential interference with a small time interval between exposures, and middle photo is the same for several minutes between exposures. Photo at right shows infinite-fringe duplication interference.

—FIG. 5

grams. Duplication interference can be obtained by superposing the reconstructed wave and a plane wave. Differential interference can be obtained by superposing the reconstructed wave on itself, with the reconstructed wave from a second hologram, or with the original object. Both single-exposure and double-exposure techniques obviously permit temporal changes to be detected and measured.

An interesting application of multiple-exposure holographic interferometry is the analysis of oscillatory motion. An oscillating system that exhibits spatially varying but temporally constant displacements will be holographically recorded as if it existed only in the positions of maximal displacement. Only at these positions will the velocity of oscillation equal zero. The resulting hologram will reconstruct an image possessing fringes that are a function of the oscillation amplitudes in the specimen.

## Perturbation detection

An alternative method of detecting perturbations of the object-illuminating wave is the image darkening such perturbations cause. Image intensity depends upon the contrast of the fringes diffracting the reconstructing wave. If the contrast of the fringes that diffract the reconstructing wave to a given image point is reduced by some perturbation during recording, that image point will be darker than if no perturbation existed. Examples of such perturbations are object motion and changes in polarization angle.

For interference to occur in holographic recording, the interfering waves must be polarized in the same plane. If the angle between the planes of polarization of  $\mathbf{U}_1$  and  $\mathbf{U}_2$  is  $\alpha$ , the intensity in the recording plane

is, by generalizing equation 1,

 $I(x,y) = |\mathbf{U}_1|^2 + |\mathbf{U}_2|^2 + |\mathbf{U}_1| |\mathbf{U}_2| \cos \delta \cos \alpha$ where  $\delta$  is the difference in phase between U1 and U2.10 Equation 1 described the situation where  $\alpha = 0$ . If  $\alpha = \pi/2$  radians, the recorded intensity becomes that of noncoherent light, and the information necessary for reconstruction is lost. Thus, if a localized area in the specimen causes α to be greater than zero, some reduction of intensity will be caused in the corresponding image area. If two reference waves with perpendicular polarization are used during recording, a comparison of intensities in the two simultaneously reconstructed images (using a single reconstructing wave) will reveal polarization effects in the specimen.17

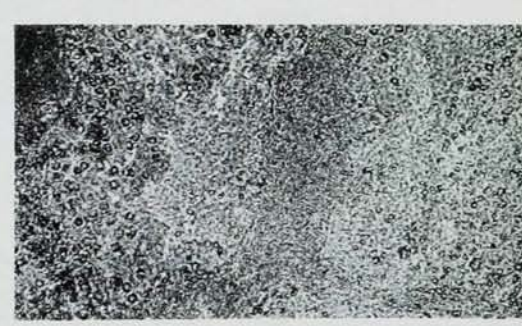
Similarly motion in the specimen will reduce the contrast of the recorded fringes. For example a fringe system with a cosine intensity,  $I = I_0$  [1 +  $\cos(2\pi \ x/S)$ ], will have an effective contrast of the form  $C = \sin(\pi \ x'/S)/(\pi \ x'/S)$ , where the spacing of the fringes is S and the displacement of the fringes during the exposure is x'. (This assumes a fictitious photographic recording medium with transmission equal to the incident intensity during recording, but it serves to illustrate the effect of fringe motion on contrast.)

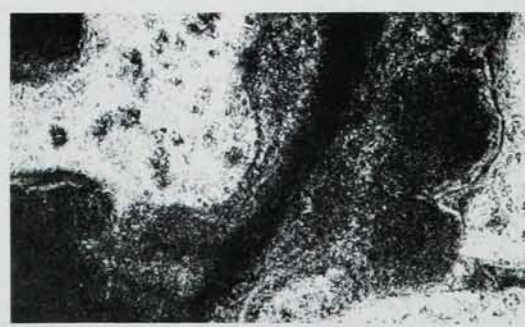
Only in highly defined systems would this effect be useful for quantitatively analyzing motion. However, it can be extremely useful for detecting and qualitatively analyzing motion in a biological specimen. Anumber of biological systems exist where the moving region consists of indistinguishable, slowly moving, or unresolvable particles (figure 6). Even when this motion can be visually

detected, it cannot be adequately recorded or spatially defined. Thus in a variety of systems (for example, cytoplasmic flow in slime molds, 10,18 neuronal secretion, mitosis and phagocytosis) motion-induced darkening can be a useful, applicable technique.

### Nonvisible illumination

Holography with nonvisible specimen illumination should be useful in specific biomedical studies for a variety of reasons. Although nonvisible illumination is used during recording, visible reconstruction retains all the characteristics of the nonvisibly illuminated specimen in the visible images.1 Holograms can be made using microwave,19 infrared, ultraviolet and acoustical20 illumination. Holography would be feasible with electrons and x rays if practical sources of coherent illumination were available. Microwaves and acoustical waves are inherently coherent; infrared lasers are more abundant than visible-light lasers. The production of coherent ultraviolet illumination might be most practical by quadrupling the frequency of a high-power visible-light or infrared laser. For example, a onestage doubling of the argon-laser frequency provides a wavelength of 253.7 nm and a two-stage doubling of the neodymium-doped-glass laser frequency provides a wavelength of 265





MOTION-INDUCED CONTRAST, demonstrated with the cytoplasmic flow in the plasmodium of Physarum connatum. At top is a conventional bright-field microscope image with laser illumination; below it is a holomicrographic image of the same specimen.

—FIG. 6

nm,<sup>21</sup> very near the absorption band of nucleic acids. Thus, in addition to providing superior resolution, ultraviolet holograms can utilize contrast based on the specific absorption of nucleic acids (260 nm) and ring-containing amino acids (280 nm).

Acoustical holography can be a useful complement both to current diagnostic ultrasonic techniques and to diagnostic radiology. These techniques respectively rely upon reflection at changes in refractive index and upon absorption. The former possesses no sensitivity to subtle changes in absorption. Acoustical holography can be tailored to detect subtle phase shifts by phase-contrast imaging, so that it can be used where current ultrasonic and x-ray techniques are not sufficiently discriminating, for example in obstetrical examinations and in the detection of breast and brain cancers.

### FILTERING AND ITS APPLICATIONS

We can use spatial filters to compare two waves (for example, to look for similarities between two cells), or we can modify a wave (for example, to improve resolution in diagnostic radiograms).

### Correlation and convolution

In holographic imaging applications, reconstruction is achieved with a reconstructing wave equivalent to the reference wave. For simplicity in reconstruction, the reference and reconstructing waves are made spherical, differing only in radius. However, nonspherical waves might be used and, as long as  $\mathbf{U}_3$  is identical to  $\mathbf{U}_1$  (equation 3), a faithful image will be formed. Moreover reconstruction can occur even if  $\mathbf{U}_3$  is not the same as  $\mathbf{U}_1$ ; the intensity of the reconstructed wave

U, Hologram f1 (x, y) f2 (x, y) Hologram  $U_4 = U_3 U_1$ f3 (x, y) U<sub>3</sub>  $U_4 = U_3 U_1$  $V_4 = V_3 \otimes V_1$ 

CORRELATION AND CONVOLUTION FILTERING. The filter is formed, as shown at top (a), by interference between the Fourier transforms  $U_1$  and  $U_2$  of a patterned reference wave  $V_1$  and a point-source object wave  $V_2$ . During the filtering operation, shown in lower part (b), the filter is illuminated by  $U_3$ , the Fourier transform of the specimen wave  $V_3$  that is to be analyzed.

—FIG. 7

will be a function of the correlation or the convolution of  $U_3$  and  $U_1$ .<sup>6,22</sup>

Consider  $\mathbf{U}_1$  and  $\mathbf{U}_2$  to be the lensformed Fourier transforms of  $\mathbf{V}_1$  and  $\mathbf{V}_2$  respectively (figure 7).  $\mathbf{V}_1$  is the wave produced by a reference specimen or pattern;  $\mathbf{V}_2$  is the wave produced by a point-source object. Furthermore, let  $\mathbf{V}_3$  be the wave produced by a sample specimen or pattern.  $\mathbf{V}_3$  is also transformed with a lens to form  $\mathbf{U}_3$ . Illuminating the hologram consisting of  $\mathbf{U}_1$  and  $\mathbf{U}_2$  with  $\mathbf{U}_3$  provides

where  $\mathfrak{F}$  denotes Fourier transform,  $\otimes$  denotes convolution and  $\bigstar$  denotes correlation. As in imaging applications, two associated waves will be produced; one is associated with  $U_2$ , the other with  $U_2^*$ . If these waves are transformed by a lens, the focal plane of the lens will contain

$$(\mathbf{V}_3 \otimes \mathbf{V}_1) \, \mathfrak{F}[\mathbf{U}_2^*] + (\mathbf{V}_3 \bigstar \mathbf{V}_1) \, \mathfrak{F}[\mathbf{U}_2] = (\mathbf{V}_3 \otimes \mathbf{V}_1) \, \mathbf{V}_2^* + (\mathbf{V}_3 \bigstar \mathbf{V}_1) \, \mathbf{V}_2$$

Thus real and virtual images of the point-source object are produced. These image points will be distributed over the two focal planes of the lens, varying in intensity as  $V_3 \otimes V_1$  and  $V_3 \bigstar V_1$  vary. Image intensity will be high where convolution or correlation is high and low where the value of these functions is low. As the convolution function is associated with real image points, it is usually the simpler to use.

# Diagnostic cytology

Correlation filtering can be applied to a variety of biomedical problems. Some examples are the selection of equivalent specimens in electron micrographs for signal-to-noise enhancement by integration, the identification of equivalent regions of nerve connections in nerve-tissue specimens, and the determination of the coördinates of malignant cells on a microscope slide. Because of the widespread interest in cancer diagnosis, this last example is the one I shall discuss.

Diagnostic cytology detects cancer by identifying malignant cells sloughed from the surfaces of body cavities. It is commonly applied to air-filled or potentially air-filled cavities such as the nose, mouth, lungs, vagina and uterus, and to fluid-containing cavities such as the chest and abdomen.<sup>26</sup> Diagnostic cytology can also be applied to fluid secretions and fluid biopsies, for example, from the breast.<sup>26</sup>

The usual technique involves spreading the specimen on a microscope slide, fixing, staining and examining the specimen through a microscope. The laborious procedure of preliminary microscopic examination might be considerably reduced by holographic correlation analysis.

Because a variety of cell configurations, orientations and aggregations are encountered in diagnostic cytology, a useful holographic filter must be multiple, consisting of a great number of component filters (figure 8). If an individual filter were made on each frame of a 35-mm movie film, over 1600 filters could be contained in 30 meters of film. At a projection speed of 16 frames per second with a 30meter filter we would require only 1 minute 40 seconds to analyze the specimen. Certainly there is no reason to limit the projection to 16 frames per second or the film length to 30 meters. The film would contain a section of "malignant" filters and a section of "benign" filters. The image plane of the filter could be scanned by a vidicon and integrated in a com-"Malignancy" correlations could be added in the computer and "benign" correlations subtracted. The output could be a cathode-ray-tube display or a typewritten set of coordinates. With a predetermined threshold for readout, only those coördinates corresponding to a specified, net "malignancy" correlation would be indicated as requiring human inspection and evaluation.

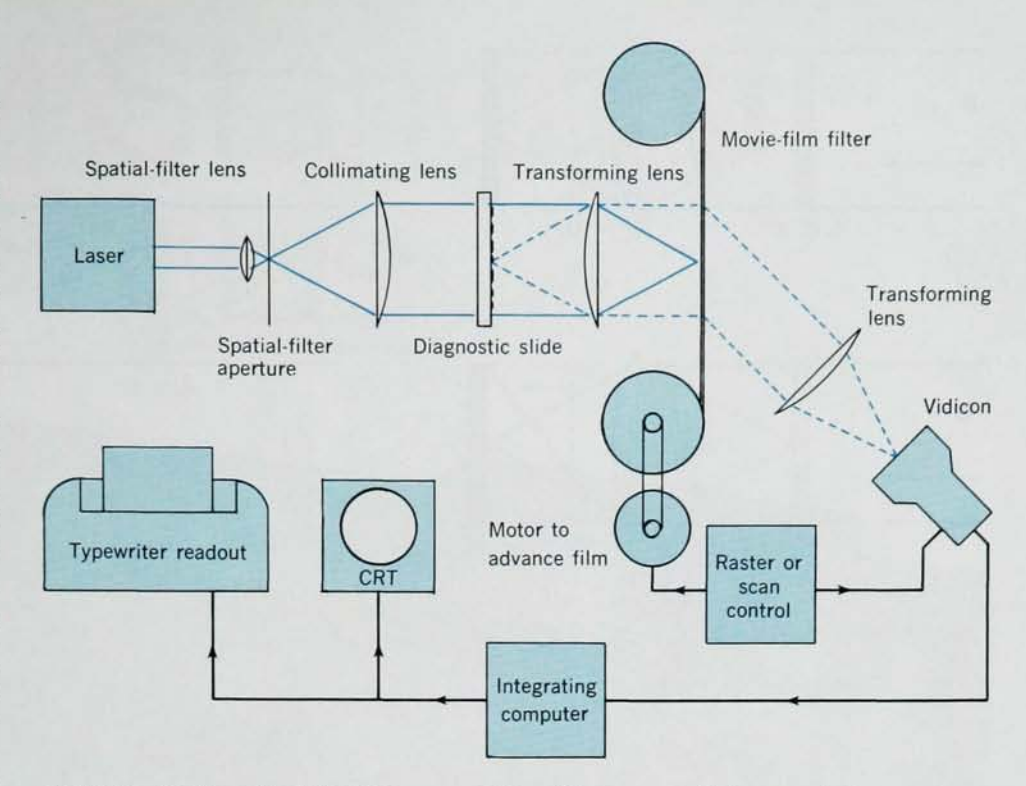
# Resolution-retrieving deconvolution

The intensity distribution in an image is not the intensity distribution predicted by geometrical optics. It is instead the convolution of the geometrical image and the spread function of the system. Thus

$$\mathbf{V}_3 = \mathbf{V}_0 \otimes \mathbf{V}_2 \tag{5}$$

where  $\mathbf{V}_3$  is the actual image,  $\mathbf{V}_0$  is the geometrical image, and  $\mathbf{V}_2$  is the spread function. The spread function can be considered as the intensity distribution in the image of a point source. In the Fourier domain, equation 5 becomes

$$\mathfrak{F}[\mathbf{V}_3] = \mathfrak{F}[\mathbf{V}_0 \otimes \mathbf{V}_2] \\
= \mathfrak{F}[\mathbf{V}_0] \bullet \mathfrak{F}[\mathbf{V}_2] \\
= \mathbf{U}_0 \mathbf{U}_2 \\
= \mathbf{U}_3$$



CYTOLOGICAL DIAGNOSIS by correlation filtering. In this suggested procedure, cancer diagnosis could be done much faster than by the present laborious technique. The cytological specimen on a microscope slide is illuminated by coherent light, and the transform of the diffraction pattern falls on separate filters on each frame of a movie film. Filtered-wave transforms are scanned and the output integrated in such a way that correlations with malignant-cell filters are added and those with benign-cell filters are subtracted. Final diagnosis can then be limited to those cells that have been located by the integrator, displayed and printed out.

—FIG. 8

If  $U_2^{-1}$  could be obtained, we could get the transform of the geometrical image wave; that is  $\mathbf{U}_3 \ \mathbf{U}_2^{-1} = \mathbf{U}_0 \ \mathbf{U}_2$  $\mathbf{U_2^{-1}} = \mathbf{U_0}.^{23,24,25}$  Because  $|\mathbf{U_2}|^2 = \mathbf{U_2}\mathbf{U_2^*}, \ \mathbf{U_2^{-1}} = \mathbf{U_2^*}/|\mathbf{U_2}|^2$ , but  $\mathbf{U_2^*}$ can be obtained holographically (equation 3) and  $U_2^2$  can be obtained photographically. Thus a deconvoluting filter, that is, a filter containing U-1, consists of two components. One contains U2\*, and the other contains |U2|-2. To form such a filter, we record V2 (figure 9). The optical system to be corrected provides Vo by forming an image of a point source on negative photographic material. A positive transparency is then obtained by contact printing. Care must be taken to ensure that  $\gamma_N \gamma_P = 2$ , where yn and yp are the gammas of the negative and positive emulsions.25

 $\mathbf{U}_2$  is obtained by illuminating the positive transparency with a plane coherent wave and transforming the transmitted wave with a lens. In the focal plane of the lens, a photographic medium will record the intensity of  $\mathbf{U}_2$ , that is  $|\mathbf{U}_2|^2$ . The transmission of this recording will equal  $|\mathbf{U}_2|^{-2}$  if the gamma of the recording equals 2.

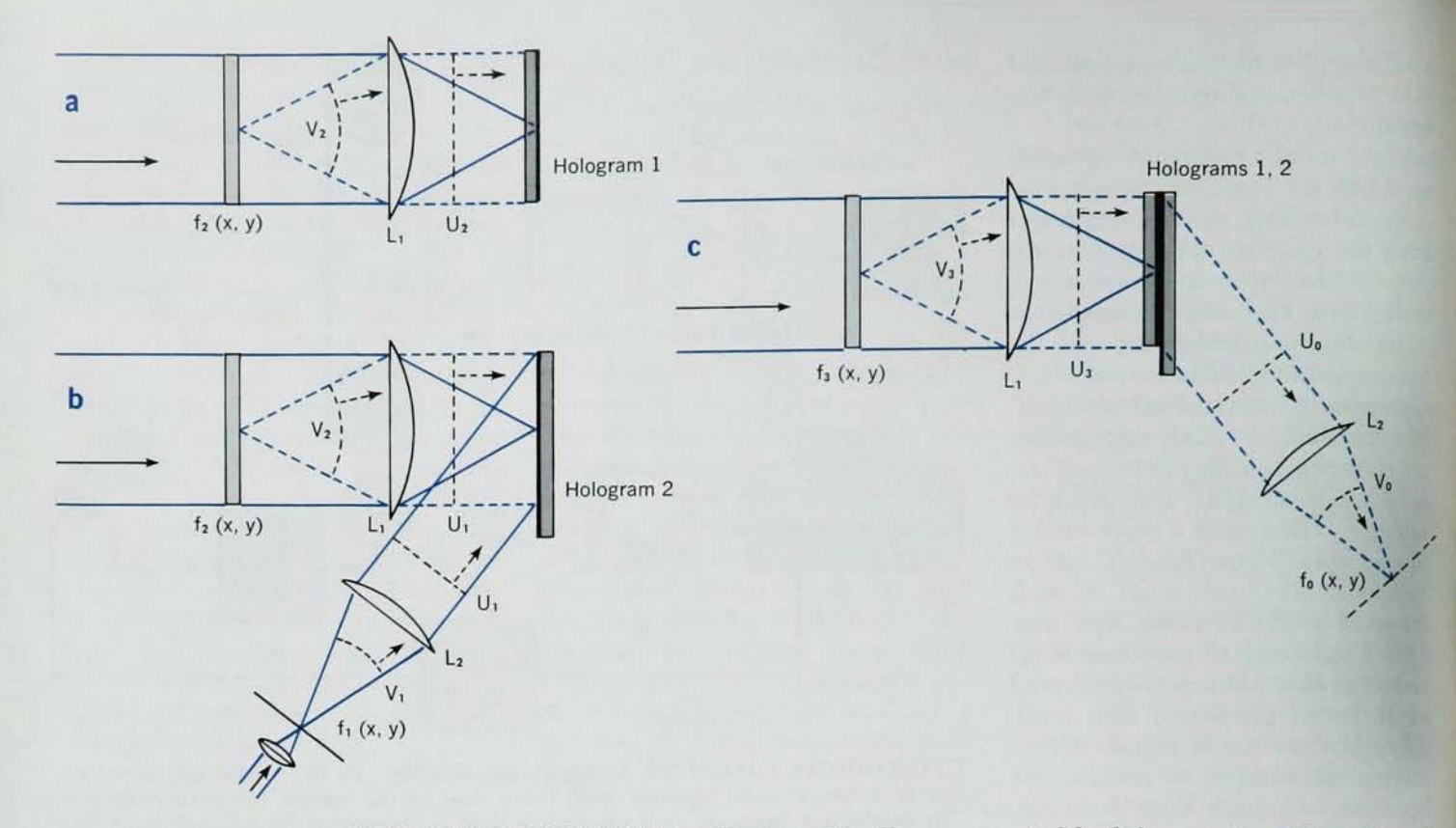
If U2 is then superimposed during

recording with a plane reference wave  $\mathbf{U}_1$  a hologram will be formed. As discussed earlier (equation 3), this hologram contains  $\mathbf{U}_2$ \*. Again, we have to process to a gamma of 2. By reversing one emulsion with respect to the other during recording, the processed plates can be sandwiched in proper registration, emulsion-to-emulsion, to form the  $\mathbf{U}_2$ \*  $|\mathbf{U}_2|^{-1}$  compound filter.

Filtering is done in a similar way to filter formation (figure 9). A positive transparency containing the image to be deconvoluted is illuminated with coherent light and transformed by a lens. In the focal plane of this lens the transformed wave  $\mathbf{U}_3$  is modulated by the filter. One of the diffracted waves is  $\mathbf{U}_3\mathbf{U}_2^* \ |\mathbf{U}_2|^{-2} = \mathbf{U}_0$ , the geometrical image.

### Diagnostic radiology

Deconvolution filtering can be applied to a variety of optical systems. Naturally it would be applicable to visible-light systems suffering from lens aberrations, or errors in lens focusing. It also could be applied to imaging systems that use electrons, infrared waves, acoustical waves or x rays. Di-



RESOLUTION RETRIEVAL by filtering. The filters represented by holograms 1 and 2 are formed by photographing the transform of a point-source image on negative material (a) and with a super-imposed reference wave (b). The two filters together (c) pass the transform of an image with improved resolution when illuminated with the transform of the image to be sharpened. The deconvoluted (sharpened) image is obtained by transforming the filtered wave.

—FIG. 9

agnostic x rays are an especially interesting potential application of this technique.

The resolution of a diagnostic radiogram is limited by the finite size of the x-ray source.<sup>27</sup> If the source, the focal spot of the x-ray tube, were a point, a perfect geometric shadow image could be formed. Because the source is not a point, the shadow is blurred or spread. In fact the image of a point object, that is a pinhole aperture, will approximate the geometrical image of the source. We can call this image the "spread function" of the system.

With a small aperture as a point-source object, a deconvolution filter  $\mathbf{U}_2^* \ |\mathbf{U}_2|^{-2}$  can be produced from an appropriately processed radiogram ( $\gamma = 2$ ). As the negative image is used in radiology, no positive is necessary. The resolution of the deconvoluted image will equal the diameter of the pinhole aperture.

Numerous advantages could be gained with these filters in radiology. First, resolution could be greatly improved. Second, with a number of different filters for specific specimenradiogram distances, three-dimensional information would be obtained as a result of selectively sharpening specific planes. Third, because resolution is no longer limited by source size, the source could be made large, thereby reducing local anode temperatures and increasing x-ray intensity. Two additional consequences of a larger source would be reduced exposure times, minimizing the risk of image-blurring due to patient motion, and increased selectivity in image focusing, that is, reduced depth-of-field in the deconvoluted image.

# References

- D. Gabor, Nature 161, 777 (1948).
- D. Gabor, Proc. Roy. Soc. (London) A 197, 454 (1949).
- E. Leith, J. Upatnieks, J. Opt. Soc. Am. 52, 1123 (1962).
- E. Leith, J. Upatnieks, J. Opt. Soc. Am. 53, 1377 (1963).
- E. Leith, J. Upatnieks, J. Opt. Soc. Am. 54, 1295 (1964).
- D. Gabor, G. Stroke, R. Restrick, A. Funkhouser, D. Brumm, Phys. Lett. 18, 116 (1965).
- D. Kozma, J. Opt. Soc. Am. 56, 1 (1966).
- 8. G. Rogers, Nature 166, 237 (1950).
- 9. M. Horman, H. Chau, Appl. Opt. 6, 317 (1967).

- 10. E. Feleppa, PhD dissertation, Columbia University (1968).
- 11. G. Ellis, Science 154, 1195 (1966).
- 12. F. Zernike, Physica 1, 43 (1934).
- R. Barer, in Physical Techniques in Biological Research (A. W. Pollister, ed.) vol. 3A, page 1, Academic Press, New York (1966).
- L. Heflinger, R. Wuerker, R. Brooks, J. Appl. Phys. 37, 642 (1966).
- R. Brooks, L. Heflinger, R. Wuerker, Appl. Phys. Lett. 7, 248 (1965).
- R. Powell, K. Stetson, J. Opt. Soc. Am. 55, 1593 (1965).
- 17. A. Lohman, Appl. Opt. 4, 1677 (1965).
- E. Feleppa, J. Cell Biol. 40, 838 (1969).
- E. Rope, G. Tricoles, J. Opt. Soc. Am. 57, 97 (1967).
- 20. A. Metherell, E. El-Sum, J. Dreher, L. Larmore, Appl. Phys. Lett. 10,
- 277 (1967). 21. F. Johnson, Electronics 39, 82 (1966).
- G. Stroke, R. Restrick, A. Funk-houser, D. Brumm, Phys. Lett. 18, 274 (1965).
- G. Stroke, R. Zech, Phys. Lett. 25, 89 (1967).
- A. Lohman, H. Werlich, Phys. Lett. 25, 570 (1967).
- 25. G. Stroke, Phys. Lett. 27, 405 (1968).
- L. Koss, Diagnostic Cytology and Its Histopathologic Bases, Lippincott, Philadelphia (1961).
- 27. K. Doi, Am. J. Roentgenol., Rad. Therapy and Nuclear Med. 94, 712 (1965).